

Spatially resolved non-invasive chemical stimulation for modulation of signalling in reconstructed neuronal networks

Yulia Mourzina, Alfred Steffen, Dmitri Kaliaguine, Bernhard Wolfrum, Petra Schulte, Simone Böcker-Meffert and Andreas Offenhäusser

J. R. Soc. Interface 2006 **3**, 333-343
doi: 10.1098/rsif.2005.0099

References

This article cites 45 articles, 4 of which can be accessed free
<http://rsif.royalsocietypublishing.org/content/3/7/333.full.html#ref-list-1>

Email alerting service

Receive free email alerts when new articles cite this article - sign up in the box at the top right-hand corner of the article or click [here](#)

To subscribe to *J. R. Soc. Interface* go to: <http://rsif.royalsocietypublishing.org/subscriptions>

Spatially resolved non-invasive chemical stimulation for modulation of signalling in reconstructed neuronal networks

Yulia Mourzina^{1,2,*}, Alfred Steffen^{1,2}, Dmitri Kaliaguine³,
Bernhard Wolfrum^{1,2}, Petra Schulte^{1,2}, Simone Böcker-Meffert^{1,2}
and Andreas Offenhäusser^{1,2}

¹*Institute of Thin Films and Interfaces, Research Center Jülich, and ²Center of Nanoelectronic Systems for Information Technology, 52425 Jülich, Germany*

³*Faculty of Chemistry, St. Petersburg State University, St. Petersburg 199034, Russia*

Functional coupling of reconstructed neuronal networks with microelectronic circuits has potential for the development of bioelectronic devices, pharmacological assays and medical engineering. Modulation of the signal processing properties of on-chip reconstructed neuronal networks is an important aspect in such applications. It may be achieved by controlling the biochemical environment, preferably with cellular resolution. In this work, we attempt to design cell–cell and cell–medium interactions in confined geometries with the aim to manipulate non-invasively the activity pattern of an individual neuron in neuronal networks for long-term modulation. Therefore, we have developed a biohybrid system in which neuronal networks are reconstructed on microstructured silicon chips and interfaced to a microfluidic system. A high degree of geometrical control over the network architecture and alignment of the network with the substrate features has been achieved by means of aligned microcontact printing. Localized non-invasive on-chip chemical stimulation of micropatterned rat cortical neurons within a network has been demonstrated with an excitatory neurotransmitter glutamate. Our system will be useful for the investigation of the influence of localized chemical gradients on network formation and long-term modulation.

Keywords: microfluidics; reconstructed neuronal networks; aligned microcontact printing (AμCP); silicon; impedance

1. INTRODUCTION

Functional coupling of nerve cells with microelectronic circuits is an important aspect of information processing and storage in bioelectronic devices, drug screening, medical engineering and biosensors. The ability to process and store large amounts of information is the most fundamental feature of the mammalian central nervous system (CNS). To accomplish this feat, the brain uses activity-dependent long-lasting modifications in synaptic strength (synaptic plasticity) (Bliss & Collingridge 1993; Kandel *et al.* 2000). Examples of such activity-dependent changes are different phases of short-term and long-term potentiation (LTP) and short-term and long-term depression. The fine organization of signal processing in neuronal circuits is not only of fundamental interest in neuroscience but also one of the key approaches for information technologies. Examples are biohybrid

systems, where defined reconstructed neuronal networks are interfaced to semiconductor-based transistor devices (Offenhäusser & Knoll 2001; Fromherz 2003). It has been shown that two-way communication by means of electrical signals between external electronics and individual neurons cultured on neurochips as well as multi-site long-term monitoring of cultured neuronal activity is possible in biohybrid systems (Pine 1980; Gross *et al.* 1997; Claverol-Tinture & Pine 2002; Merz & Fromherz 2005).

One side of this interface, the electronic circuitry, has witnessed substantial progress. Planar arrays with large number of electrodes or field-effect transistors per unit area (Eversmann 2003; Kaul 2004) as well as new electrode and gate materials (Egert 1998) have been put into practice. On the biological side, studies on reconstruction, modulation (geometry, polarity (Oliva 2003; Vogt 2004), synaptic strengths of individual synapses) and signal processing properties of reconstructed neuronal networks are essential prerequisites for the realization of a neuroelectronic concept (Neher 2001). Investigations of these phenomena can be

*Author and address for correspondence: Institute of Thin Films and Interfaces, Research Center Jülich, Jülich 52425, Germany (y.mourzina@fz-juelich.de).

approached by employing miniaturized systems for cell molecular biology studies and cell manipulations. Examples are:

- (i) *in vitro* electrophysiological experiments. On-chip stimulation and activity recording of neuronal cells as well as studies on ion-channels expressed in cell lines (Gross *et al.* 1997; Offenhäusser & Knoll 2001; Claverol-Tinture & Pine 2002; Brüggemann *et al.* 2003; Fromherz 2003; Otto *et al.* 2003; Stetts *et al.* 2003; Berdondini *et al.* *in press*) have been demonstrated;
- (ii) cell culture and cell manipulations in microfluidic systems. In particular, cell guiding and reconstruction of neuronal circuits on solid substrates have been achieved by means of chemical (Folch & Toner 2000; Chang *et al.* 2001; Vogt *et al.* 2005), topographical (Maher *et al.* 1999; Folch & Toner 2000; Sugio *et al.* 2004), magnetic field (Eguchi *et al.* 2003) and optical (Mohanty *et al.* 2005) guidance. Also the formation of *in vitro* neuronal circuits has been demonstrated by combining topographical barriers (microfluidic structures) with the immobilization of cell adhesive substances inside microfluidic channels (Morin *et al.* 2005; Rhee *et al.* 2005). Most studies on cell positioning in microfluidic systems have been performed with non-adherent cells from cell lines due to easier handling; and
- (iii) genomics/proteomics/metabolomics cellular analysis (Li *et al.* 2002; Aebersold & Mann 2003; Lion *et al.* 2003; Lu *et al.* 2004; Peng *et al.* 2004; Issaq *et al.* 2005; Mourzina *et al.* 2005) and transfection assays (Szili *et al.* 2004; Matsue 2005; Nagamine *et al.* 2005). These biochemical approaches will help to correlate the alterations at the electrophysiological level with those at the biochemical level. For example, the action of a modulation factor for feedback connections and molecular engineering of cellular signal amplification cascades can be investigated (Neher 2001).

Signal processing pathways in the central nervous system can be modified through persistent alterations in the efficacy of synaptic connections, which are based on the activity patterns. In 1973, the effect of brief trains of high frequency stimulation on the monosynaptic excitatory pathway in the hippocampus was found to cause a sustained increase in the efficiency of synaptic transmission (Bliss & Gardner-Medwin 1973). This effect is referred to as LTP, and is accompanied by 'some growth or metabolic changes' (Hebb 1949; Kandel *et al.* 2000). Later on, biochemical modulation of the efficacy of synaptic communication by agonists and antagonists of membrane receptors was shown (Bortolotto *et al.* 1994; O'Connor *et al.* 1994). Therefore, long-term activity-dependent modifications of synaptic connections of neighbouring cells might allow the modulation of signalling in reconstructed networks of biohybrid systems. It is desirable to

perform this task in an addressable manner and with spatial resolution on a single cell level. Additionally, it is important to reproduce non-invasive natural biochemical stimulation/inhibition conditions to study plasticity over time periods of days and longer. Patch clamp analysis is generally necessary at different stages of the system development and validation. This method remains the most precise technique for electrophysiological investigation of ion-channels. However, large micromanipulators required to hold a pipette and perfusion system make simultaneous recordings of more than one neuron difficult. Therefore, it is also advantageous to integrate a system for the delivery of substances in the substrate upon which neurons are cultured.

The first devices for the manipulation of the extracellular environment of neuronal cells were designed as implantable probes for *in vivo* studies (Ludvig *et al.* 1994). However, they are not applicable to interface reconstructed neuronal networks on planar substrates. Nevertheless, the microfluidic approach can be adopted to design on-chip delivery systems. A solid-state silicon microchip that can provide a controlled release of single or multiple chemical substances on demand has been described by Santini *et al.* (1999). The release mechanism is based on the electrochemical dissolution of thin anode membranes ($50 \times 50 \mu\text{m}^2$ area) covering microreservoirs. The reservoirs extended completely through the wafer and were filled with chemicals in liquid, gel or solid form. Release from a particular reservoir was initiated by applying an electrical potential between the anode membrane covering that reservoir and a cathode. The system was tested with a prototype microchip using gold and saline solution as a model electrode material and release medium. However, it was noted that the presence of small amounts of chloride could create an electric potential, which favoured the formation of soluble gold chloride complexes. This circumstance is not favourable for applications of the device in real cell culture media, which contain millimolar concentrations of chloride ions. Other metals such as copper and titanium were reported to be unsuitable under the conditions of the experiment.

The concept mentioned above has been advanced by Peterman *et al.* (2004) and Takoh *et al.* (2005). They developed a porous membrane-based substrate to provide localized chemical release of substances to cultured cells via a microfluidic interface from below. Intercellular communications of cardiac myocytes cultured on porous polycarbonate membranes (Takoh *et al.* 2005) were detected by observing cytosolic Ca^{2+} transients using fluo-4. The same detection method was employed to observe repeated stimulation of PC12 cells with bradykinin (Peterman *et al.* 2004). In these experiments, the PC12 cells were cultured on silicon nitride membranes integrated into silicon chips.

An on-chip gradient generating microfluidic device for pharmacological profiling has been described by Pihl *et al.* (2005). The device allows generation of concentration gradients spanning nearly five orders of magnitude and demonstrates the integration of on-chip gradient generation with the concept of open-volume

microfluidics. The performance of the system is demonstrated by pharmacological screening of the voltage-gated K^+ channels (hERG) and ligand-gated GABA_A receptors expressed in cell lines. A disadvantage of the system for neuronal cell studies is that each cell should be translated to the exit of the channels after it is patch-clamped in the open-volume. Such manipulations are not adequate for cortical neurons, which are connected in networks and adhere with their cell bodies and branched trees of neurites to polylysine/extracellular matrix (PL/ECM) coated patterns.

In this work, we attempt to design cell-cell and cell-medium interactions in confined geometries with the aim to manipulate the activity patterns of individual neurons in on-chip reconstructed neuronal networks. This approach may be adapted to induce long-term activity-dependent changes at a particular synapse in the network. We describe a biohybrid microfluidic system with geometrically defined reconstruction of neuronal networks on silicon chips. The cells are aligned with the features on the chip surface, where a neurotransmitter solution can be applied to the micropatterned cell culture in a controlled way. A planar on-chip concept also allows for the integration of further functional elements within a device (e.g. liquid actuation, additional electrical stimulation and recording functions) by means of standard semiconductor technologies. Silicon substrates, although preventing observation by many techniques of microscopy, allow for miniaturization and integration of electronic circuits, which is important for the development of bioelectronic, biosensor and neuroprosthetic devices. We present the design and fabrication of the chip as well as results of the experiments with reconstructed networks of embryonic rat cortical neurons.

2. MATERIALS AND METHODS

2.1. Preparation of silicon substrates

The structures were prepared in a class 100 clean room by means of double-side alignment photolithography in combination with anisotropic wet chemical etching, as schematically shown in figure 1. Silicon wafers were cleaned using the RCA protocol. Subsequently, silicon oxide and silicon nitride layers were deposited by thermal oxidation and low-pressure chemical vapour deposition, respectively. At first, one side of the wafer was patterned by means of photolithography with a positive photoresist UV 6-06. Reactive ion etching was used to remove the exposed silicon nitride and oxide patterns as well as the remaining photoresist. The second side of the wafer was structured following the same procedure. Afterwards, anisotropic chemical wet etching in 22% potassium hydroxide at 80 °C was employed to create suspended silicon nitride membranes with microapertures, figure 1e. Silicon nitride layers grown on silicon were not stable enough to serve as a mask layer during chemical wet etching of silicon due to the mechanical stress of the material. Therefore, a silicon oxide layer was required to compensate the mechanical stress of silicon nitride, thereby improving stability and adhesion of the mask layer. The size of the

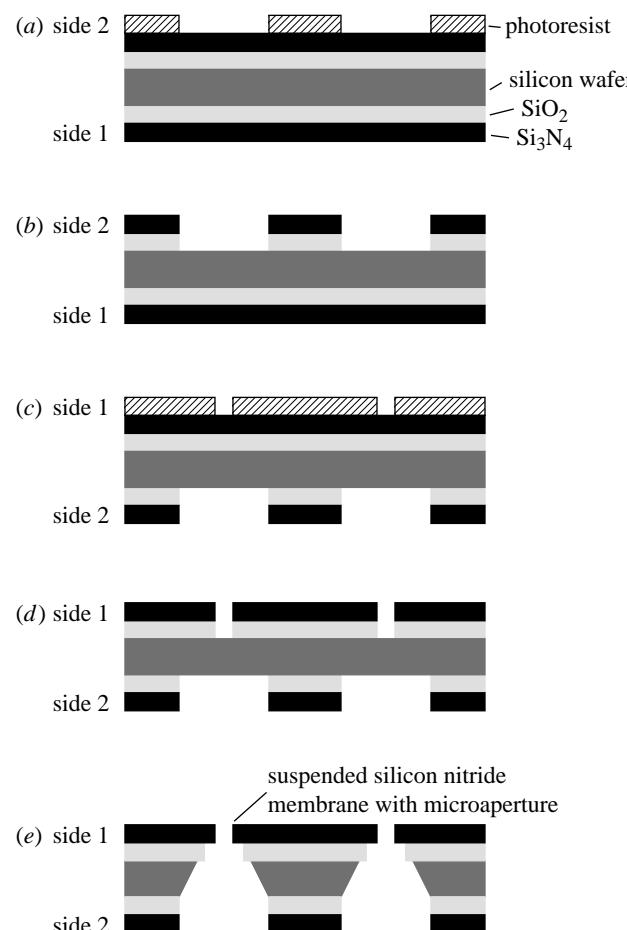


Figure 1. Fabrication process of silicon substrates with suspended membranes containing microapertures: (a) deposition of silicon oxide and silicon nitride layers on a double-side polished silicon wafer followed by photolithography, (b) reactive ion etching (RIE) of silicon nitride, silicon oxide, and photoresist, (c) double-side alignment photolithography, (d) RIE of silicon nitride, silicon oxide, and photoresist and (e) anisotropic wet chemical etching.

microapertures varied from 1 to 9 μm , both circular and quadrangular geometries of the microapertures were tested, figure 2. Each chip contained apertures, which were uniform in size and geometry. The chips were used for culturing neuronal cells.

2.2. Preparation of the microfluidic system based on poly(dimethylsiloxane)

A microfluidic system of poly(dimethylsiloxane) (PDMS) elastomer was prepared by soft lithography (Mourzina *et al.* 2005). Masters for soft lithography were fabricated mechanically with different materials: Teflon, aluminium, steel. However, no dependence of the mould materials on microreplication was observed. The height of the raised structure on the master, which corresponds to the channel pattern, was 500 μm . A mixture (Sylgard 184) of elastomer precursor and its curing agent were degassed, poured over the master and cured at 65 °C for 4 h. After curing, a soft elastomer copy was peeled-off the master and could be sealed to the planar surface of a non-structured PDMS plate. A flat PDMS plate was prepared as described above

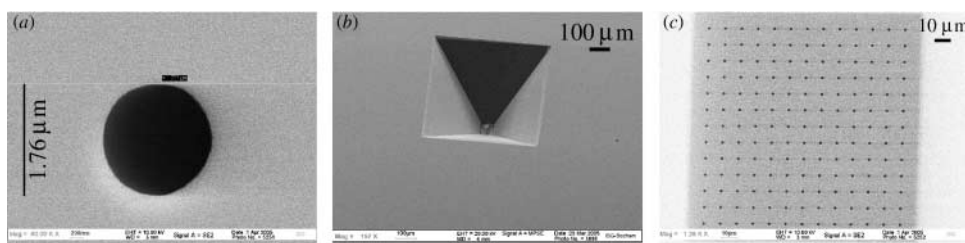


Figure 2. SEM images of the silicon chips with suspended membranes containing microapertures: (a, b) single microapertures in a suspended membrane, (c) multiple microapertures in a suspended membrane, (a, c) view from the top of the chip, (b) view from the bottom of the chip.

using a non-structured silicon wafer as a master. To make the connections of the microfluidic system to the pump, the syringe needles were inserted into the PDMS channels before irreversibly bonding two PDMS plates. The opposite side of the cannula was cut and inserted into the tubes. The tubes were connected to the syringe pump (World Precision Instruments). Syringe needles of 450 μm diameter were used.

2.3. Preparation of the device

The final device was assembled of three parts. The bottom part was a PDMS microfluidic system (figure 3a) connected to a syringe pump and a waste reservoir, as described in §2.2. The chip (without cell culture for microfluidic experiment or with cell culture) was placed on the microfluidic part and covered with a 24 \times 24 mm^2 printed circuit board (PCB) of 1 mm thickness. The PCB has an opening of 9 mm diameter in the middle. A glass ring with a diameter of 17 mm was glued onto the upper surface of the PCB by means of a thin PDMS layer. The whole assembly was aligned and fixed. The device was able to hold 1 ml of extracellular solution for patch-clamp experiments. A photograph of the chips (1 cm^2) and the assembled device is shown in figure 3b.

2.4. Characterization of the structures (optical, electrochemical, microfluidic)

The structural features and geometry of silicon chips were characterized by reflected and transmission light microscopy (POLYVAR MET, Leica), and scanning electron microscopy ('GEMINI 1550', LEO). Scanning electron microscopy (SEM) images of silicon chips are shown in figure 2.

Impedance characterization of the structures was performed by means of dc (283 Potentiostat/Galvanostat, EG&G Princeton Applied Research) and ac (1260 Impedance/Gain Phase Analyzer, Solartron) measurements. For the measurements, the backside of the chip was contacted via liquid junction to an Ag/AgCl electrode. The measurements were performed in extracellular electrolyte solution 1 (ES1) (see §2.5 for the composition), figure 4a-c. The data were fitted using the equivalent circuit model presented in figure 4d.

Flow via microapertures in the assembled devices was characterized by: (i) optical microscopy with a solution of a brilliant blue dye, and (ii) measuring the changes of the bulk potassium ion concentration on the

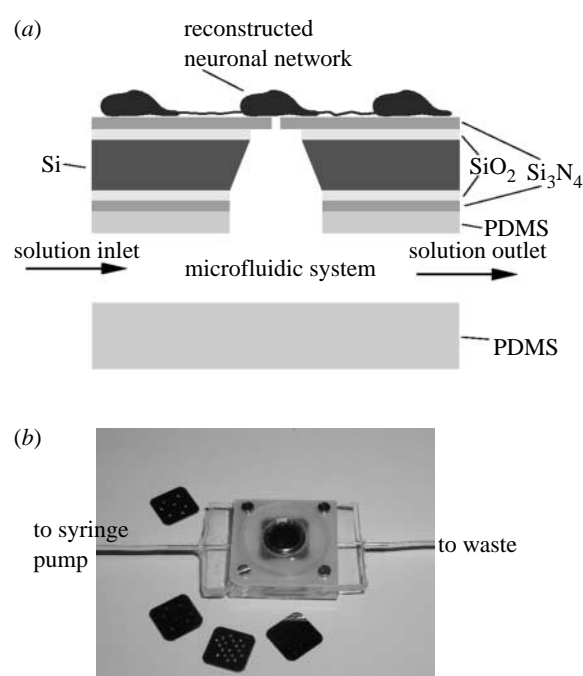


Figure 3. (a) Schematic of the interface between a PDMS microfluidic system and neuronal networks reconstructed on silicon chips and (b) a photograph of the assembled device.

chip surface due to the delivery of potassium ions via the microfluidic system.

For the latter experiment, a K^+ -ion-selective electrode (K^+ -ISE) was prepared using the membrane composition described earlier (Mourzina *et al.* 2003). The diameter of the K^+ -ISE membrane was 7 mm. As a reference electrode, an Ag/AgCl wire electrode was prepared. The sensitivity of the K^+ -ISE was $56 \text{ mV} (\lg C_{\text{K}^+})^{-1}$ in the concentration range $3 \times 10^{-3} \text{--} 10^{-1} \text{ M K}^+$. As background electrolyte for the sensitivity measurement we used ES1 (see §2.5 for the composition). For the characterization of flow, 1 ml of ES1 (containing 3 mM KCl and constant concentration of chloride ions of 129 mM) was placed on the chip surface of the assembled device. The extracellular solution (ES1) with a higher concentration of potassium ions (100 mM) was prepared by addition of potassium nitrate to keep the concentration of chloride ions constant. The latter solution was delivered onto the chip surface of the assembled device via the microfluidic system and the microapertures. Increase in the bulk concentration of potassium ions could be followed by changes in the response of the K^+ -ISE.

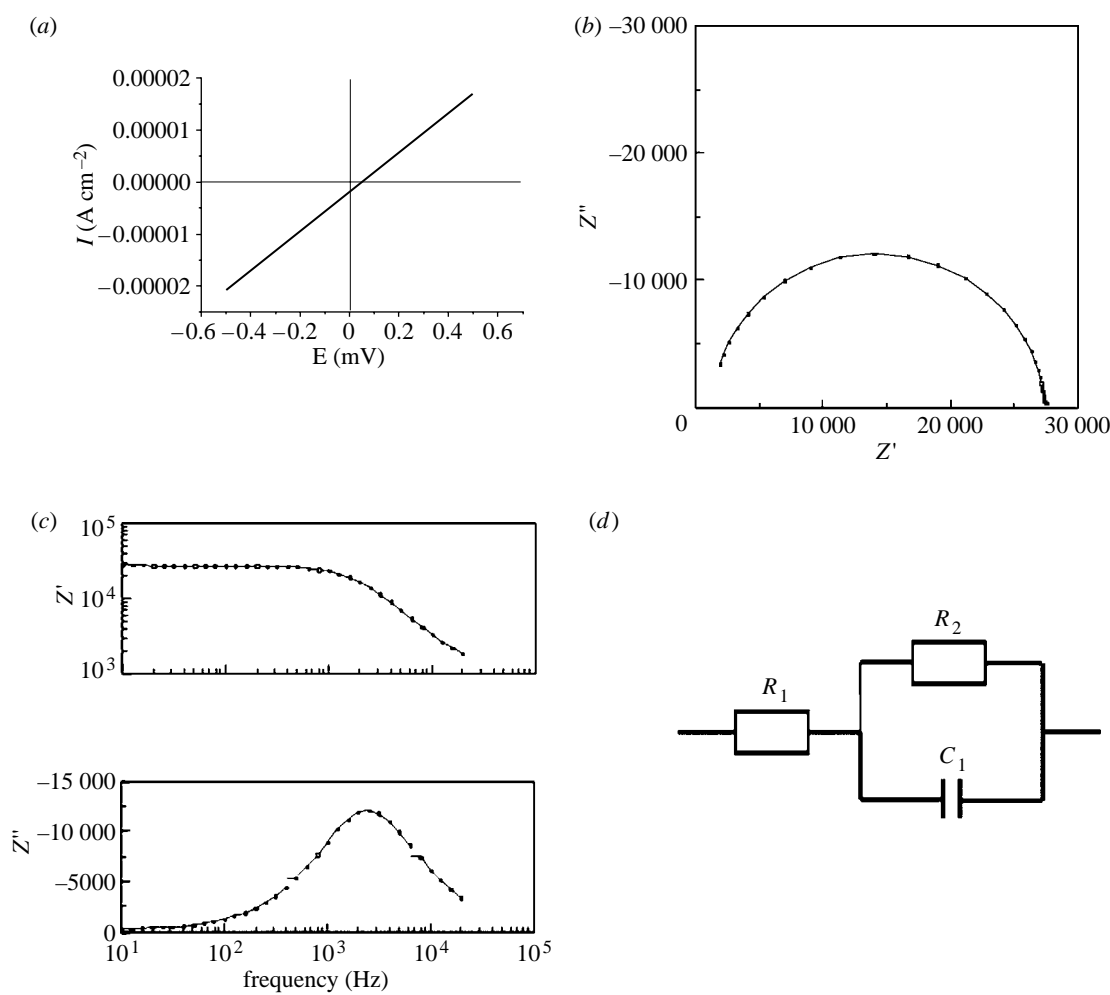


Figure 4. Impedance characterization of the structures: (a) a direct current experiment, (b, c) alternating current measurements, (d) an equivalent scheme to calculate the resistance and capacitance of the structures. The measurements for the structure containing one square $7 \times 7 \mu\text{m}^2$ ($A = 49 \mu\text{m}^2$) aperture are shown. The measurements have been performed in extracellular solution (ES1). R_1 corresponds to the resistance of the electrolyte filled measurement cell; R_2 is the resistance of the chip dominated by the electrolyte filled microstructures; C_1 represents the capacitance imposed by the chip and the silicon nitride membrane. R_1 was measured to be 460Ω .

2.5. Reconstruction of neuronal networks on silicon chips by means of aligned microcontact printing technique (μCP)

Before culturing cells on the chip surfaces, the chips were made hydrophilic and cleaned. A hydrophilic chip surface was achieved by treatment with $\text{H}_2\text{O}_2 : \text{H}_2\text{SO}_4$ (1 : 2 vol.parts) for 20 min followed by intensive rinsing with deionized water. The chips were then immersed in a solution of 70% ethanol or alternatively heated to 200 °C for 3 h. Both procedures were found to be adequate for sterilization.

Geometrically controlled reconstruction of neuronal networks was achieved by microcontact printing as described in detail before (Vogt *et al.* 2004). For this purpose, microstamps with grid structures were fabricated by curing PDMS in 2 ml Eppendorf tubes upside down on a master stamp produced by photolithography. Alternatively, flat PDMS stamps of about 1–2 mm thickness were prepared using the same master mould. The grid structures had meshes of $50 \mu\text{m} \times 100 \mu\text{m}$, somal adhesion sites of $22 \mu\text{m}$ diameter, and lines of $4 \mu\text{m}$ width. Patterning was performed with the aid of a

xy-positioning system (Fineplacer 96, Finetech, Germany) by first inking the microstamp for 30 s in a 1 : 100 dilution of ECM-gel (Sigma, Germany) in Dulbecco Modified Eagle's Medium (Invitrogen, Germany) containing $25 \mu\text{g ml}^{-1}$ poly-D-lysine (PL), molecular weight 70.000–150.000 t (Sigma, Germany). Then the surface of the stamp was dried in a stream of nitrogen. The stamp was immediately attached to the stamp holder of the *xy*-positioning system, and after alignment of the stamp micropattern with the microapertures of the silicon chip, pressed to the chip for 20 s. Embryonic rat cortical neurons were subsequently plated on the patterned substrates and cultured as described below.

Rat embryonic cortical neurons were obtained as described previously (Brewer *et al.* 1993). Briefly, embryos were recovered from pregnant Wistar rats at 18 days gestation (E18). The cortex was dissected from the embryonic brain, cells were mechanically dissociated by trituration in Hank's Balanced Salt Solution (HBSS) (without Mg^{2+} and Ca^{2+} , GIBCO 14170-088), 0.035% sodium bicarbonate, 1 mM sodium pyruvate, 10 mM HEPES, 20 mM glucose, pH 7.4 with a fire

polished siliconized Pasteur pipette. Two volumes HBSS (GIBCO 24020-091) 0.035% sodium bicarbonate, 1 mM sodium pyruvate, 10 mM HEPES, 20 mM glucose, pH 7.4 were added. Non-dispersed tissue was allowed to settle for 3 min. The supernatant was centrifuged at 1100*g* for 2 min. The pellet was resuspended in 1 ml Neurobasal (NB) Medium (GIBCO 21103-049), 1× B27 (GIBCO 17504-044), 0.5 mM L-glutamine (GIBCO 35050-038) per hemisphere isolated. An aliquot was diluted with trypan blue solution and dye-excluding cells were counted in a Neubauer chamber. The remaining cells were diluted in NB medium with the above supplements and plated onto the μ CP silicon substrates at a density of 16 000 cells cm^{-2} . Half of the culture medium was replaced with fresh growth medium every 3–4 days. The cells were maintained in a 37 °C humidified incubator with 95% air and 5% CO_2 .

Electrophysiological characterizations were performed using a patch-clamp set-up (HEKA Elektronik, Germany) in the whole-cell configuration in current-clamp mode and voltage-clamp mode, typically at 10–14 days *in vitro* (DIV). Borosilicate micropipettes (Hilgenberg, Germany) with a resistance of *ca* 8 M Ω were pulled using a micropipette puller (P-97, Sutter Instrument Company, CA, USA). In the case of electrical stimulation, both voltage-clamp and current-clamp recordings were performed. In the voltage-clamp mode, the cells were stimulated with 50 or 100 ms voltage changes from −100 to +100 mV with a step of +10 mV. The voltage-clamp recordings were made at a holding potential of −70 or −65 mV. In current-clamp mode, the cells were stimulated with −100–700 pA current pulses with a step of 50 pA. For the experiments on chemical stimulation, the protocol was changed, so that only recordings of the membrane potential were performed and no electrical stimulus was applied. The ES1 contained, mM: 120 NaCl, 3 KCl, 1 MgCl₂, 2 CaCl₂, 10 HEPES, pH 7.3 adjusted with 1 M NaOH. The extracellular solution 2 (ES2) was prepared using the same formulation without addition of magnesium, instead, glucose and glycine were added at 1 mM and 5 μM , respectively. The intracellular solution contained, mM: 2 NaCl, 17.5 KCl, 0.5 MgCl₂, 5 HEPES, EGTA 0.2, 118 potassium gluconate, 4 ATP, pH 7.3 adjusted with 1 M KOH.

2.6. Cell–medium interactions in confined geometries: chemical stimulation of neuronal cells on microfluidic devices

Patch-clamp recordings have been performed to observe the response of cells to the chemical stimulus delivered via the microfluidic system using recording protocols without electrical stimulation. Stimulation solutions of glutamate 1 and 10 mM were prepared using ES2 as a background solution. pH of the solutions was controlled and adjusted with sodium hydroxide, if necessary. After delivery of the stimulation solution, the inward syringe needle of the microfluidic system was connected to the supply of the extracellular solution (ES1). The extracellular solution was delivered onto the chip surface replacing the glutamate containing solution, which was simultaneously sucked from the

chip surface. Afterwards, normal patch-clamp recordings of the cells were performed to examine that the cells on-chips did not die due to excitotoxic effect of glutamate.

3. RESULTS

Images in figure 2 demonstrate that a good precision in positioning the structural features on the opposite sides of the wafers can be achieved by means of double-side alignment photolithography and anisotropic wet chemical etching of silicon (figure 2). No differences in the quality of the structures have been observed for two different geometries of the microapertures (circular or square). In the initial design of the chip, the neighbouring distance between the larger apertures was 1–3 mm (figure 2a,b) to guarantee the stability of the suspended membrane. Only one aperture was structured on each suspended membrane. We found that suspended membranes with a higher density of apertures were also stable. An example of such an array of apertures on a suspended membrane is shown in figure 2c, where the distance between the smaller apertures is less than 10 μm . These multiple apertures cannot be addressed individually and provide multiple chemical ejection sites. In the present work, we used the structures with one microaperture in each suspended membrane, which can provide a single chemical ejection site. A higher density of the individual stimulation sites can be achieved by using thinner silicon wafers.

To guarantee normal conditions for cell culture, the cell culture substrate is detachable from the microfluidic part of the device and the PCB cover. An additional advantage of such a modular assembly is that no epoxy gluing and encapsulation processes of the PCB are necessary. Culturing cells on the chips can be performed following standard protocols without minimizing the volume of cell–medium.

Characterization of the impedance of the structures is shown in figure 4 for the device assembly containing one square $7 \times 7 \mu\text{m}^2$ ($A = 49 \mu\text{m}^2$) aperture. The data were used to calculate the resistance and capacitance of the chip using an equivalent circuit model shown in figure 4d. R_1 was found from I–V measurements carried out in the measurement cell without a chip and kept as a constant parameter in the fitting procedure. The relative standard deviation of measurements for chips with the same size and geometry of the apertures was found to be less than or equal to 6% ($n = 5$ and $p = 0.95$, where n is the number of chips tested and p is the confidence coefficient). In table 1, the data for two chips with different aperture numbers and geometries are compared. In extracellular medium, the resistance of the structure was found to be tens of kilohms and the capacitance was about 2 nF. Good correlation between the data is observed.

Experiments were performed to characterize and estimate the velocity of the transfer of the substance from the microfluidic part onto the chip surface, as exemplified in figures 5 and 6. Figure 5 shows microscope images taken at a rate of 1 per second. The flow rate was 0.03 ml min^{−1} (controlled by a syringe pump). It is important to notice that the

Table 1. Impedance characterization of the structures. (The data were calculated using the model presented in figure 4d. The measurements were performed in extracellular solution (ES1), r is the radius of the circle aperture, and a is the size length of the square aperture, A is the aperture area.)

	chip 1; 9 circle apertures, $r=2.5\text{ }\mu\text{m}$; area of the apertures, $A=177\text{ }\mu\text{m}^2$	chip 2; 1 square aperture, $a=7\text{ }\mu\text{m}$; area of the aperture, $A=49\text{ }\mu\text{m}^2$
R_1 fixed, $460\text{ }\Omega$		
$R_2, \text{ k}\Omega$	9.44 (ca $85\text{ }\text{k}\Omega$ per aperture)	26.25
$C_1, \text{ nF}$	2.26	2.20

solution, which was delivered via a large microaperture ($9\text{ }\mu\text{m}$), is localized in a confined area on the chip surface even 14 s after its appearance. This observation shows that the localized delivery of substances onto the chip surface for the purpose of localized chemical stimulation of cells or creation of chemical gradients on the chip surface is possible with the system. The localized area progressively increases with time. However, this increase does not obey a linear dependence on time, but becomes slower after initial delivery of a substance onto the chip surface. The localized area becomes larger with increasing flow rate.

The transfer of the substance from the microfluidic part onto the chip surface was characterized as described in §2.4. The rate of delivery was estimated to be $50\text{--}90\text{ nl}(\text{s aperture})^{-1}$ for a flow rate of 0.3 ml min^{-1} . This variation is probably explained by diffusion processes on the chip surface, the response time of the K^+ -ISE, and the difficulty to control the flow in a multi-level microfluidic system with a syringe pump. It is important to note that the method described allows us to estimate the bulk changes in the activity of potassium ions in the solution on the chip surface. Therefore, higher flow rates were used in these experiments (typically, $0.1\text{--}0.3\text{ ml min}^{-1}$) than in the experiments described above (figure 5). Due to concentration gradients shown in figure 5, the concentration at the localized area in the vicinity of the delivery aperture is higher than the bulk concentration measured by the ion-selective electrode. In some cases, peaks in the response of the electrode were observed, as illustrated in figure 6b. This sudden increase in potassium ion concentration may be related to non-precise positioning of the K-ISE or non-uniform filling of the volume under the chip surface.

Figure 7a,b show microscopy images of a PL-FITC pattern on the silicon nitride surface as well as a PL/ECM pattern on the chip surface prepared by A μ CP with the aid of a xy -positioning system, as described in §2.5. The cortical neuronal cells were plated on such substrates and cultured as described in §2.5. Figure 7c shows a microscopy image of the cell culture at day 14. The networks of patterned neurons are ordered in lines following the PL/ECM traces on the substrate surface. Individual cell bodies were between 10 and $15\text{ }\mu\text{m}$ in diameter. The arrow shows an example of a cell body and a neurite growing in the proximity of the aperture. The electrophysiological properties of the cells growing on the geometrically defined PL/ECM patterns on silicon chips were characterized by means of patch-clamp studies, figures 8a,b. The cells in the

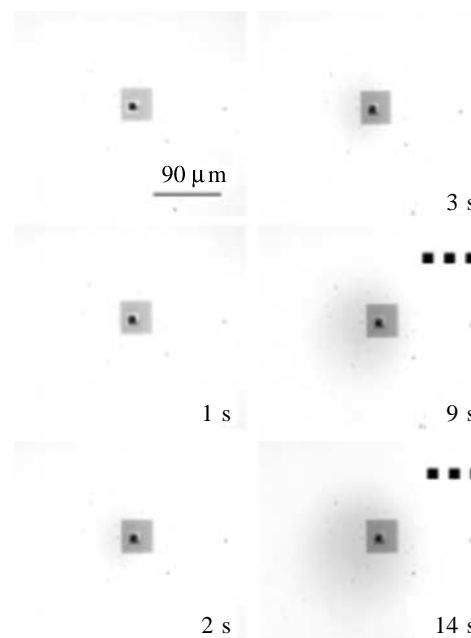


Figure 5. Optical visualization of flow via the microfluidic system: (a) flow rate of a syringe pump was 0.03 ml min^{-1} , diameter of the aperture was $9\text{ }\mu\text{m}$. A dye (saturated solution of brilliant blue filtered through a $0.2\text{ }\mu\text{m}$ filter) was used for visualization of the flow.

reconstructed neuronal networks preserve electrophysiological properties and generate action potentials in response to electrical stimuli, as it is illustrated in the figure. Therefore, the system was further validated with neurotransmitter glutamate as a main excitatory neurotransmitter in the CNS.

Electrophysiological recordings of the neuronal cell, which is marked with an arrow in figure 7c, are shown in figure 9a. At first a normal stimulation protocol was applied. After recordings, which showed normal electrophysiological behaviour of the cell, the delivery of extracellular solution containing glutamate and glycine via the microfluidic system was initiated and the membrane potential of the same cell was monitored using a modified protocol (§2.5, a protocol without applying an electrical stimulus), figure 9b. In figure 10a,b, the results of similar experiments are shown. After delivery of glutamate, the inward syringe needle of the microfluidic system was connected to the supply of the extracellular solution (ES1). The latter was delivered onto the chip surface replacing the glutamate containing solution, which was simultaneously sucked from the chip surface.

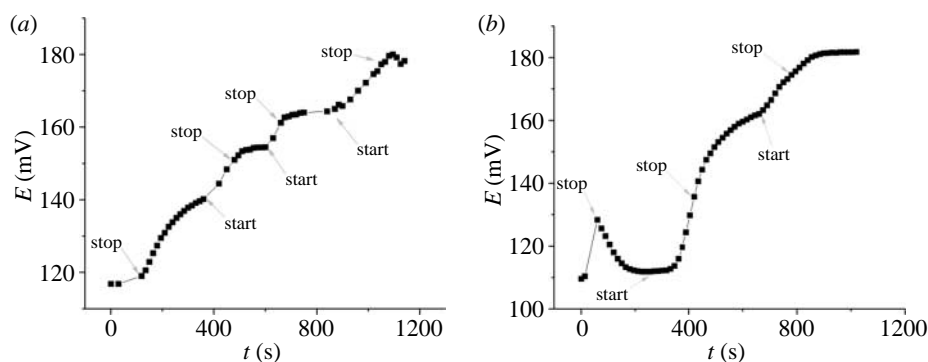


Figure 6. Characterization of the flow via the microfluidic system and microapertures in the assembled device as measured with a K^+ -ISE; stop and start mark the times, when the syringe pump was switched off and on, respectively. Flow rate was 0.3 ml min^{-1} .

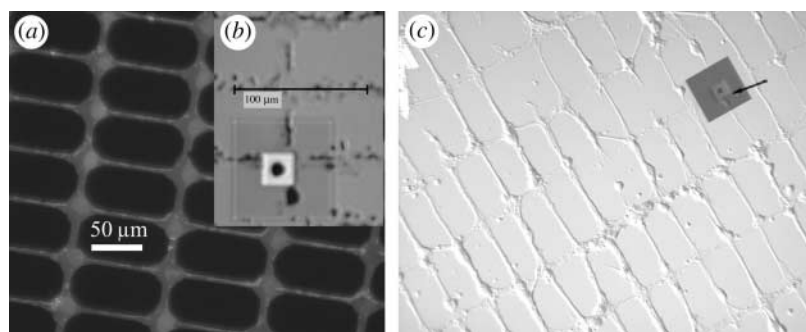


Figure 7. (a) A fluorescence microscopy image of a pattern of PL-FITC on the silicon nitride surface, (b) a microscopy image of a PL/ECM pattern on the chip surface prepared by means of $\text{A}\mu\text{CP}$ using a xy -positioning system, and (c) a microscopy image of the cell culture at day 14 (DIV 14), cells on the silicon chip have been guided by means of $\text{A}\mu\text{CP}$ with PL/ECM.

4. DISCUSSION

After delivery of the neurotransmitter to the chip surface, the cell generated a burst of action potentials, and depolarization of the cell membrane was observed, as shown in figure 9b. These observations can be explained by activation and opening of ionotropic glutamate receptors (a-amino-3-hydroxy-5-methylisoxazole-4-propionic acid (AMPA), kainate, N-methyl-D-aspartate (NMDA)) due to chemical stimulation with a neurotransmitter.

In the experiment shown in figure 10a, the cell was spontaneously active and fired action potentials without being stimulated electrically. It is interesting to observe the changes in the spontaneous activity patterns during recording, which is caused by the delivery of glutamate via the microfluidic system. This change in the activity pattern correlates with the slow deactivation kinetics of NMDA glutamate receptor channels with NR2B subunits (50–500 ms) (Fox *et al.* 1999; Cull-Candy *et al.* 2001; Popescu & Auerbach 2004), which is activated in the presence of the co-agonist glycine. In general, we observed three main types of responses in our experiments on on-chip chemical stimulation with the system described: generation of action potentials, changes in the kinetics of spontaneously active neuronal cells and generation of excitatory potentials similar to post-synaptic potentials. These variations in the responses of cells can be explained by different factors, such as the amount of glutamate molecules binding to the receptors, the number of post-synaptic receptors of the cell, and the

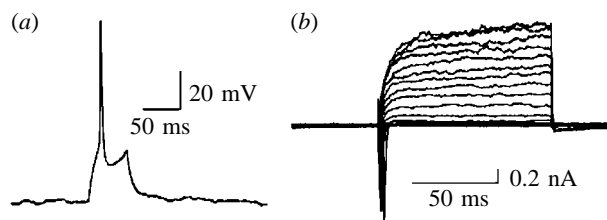


Figure 8. Electrophysiological characterization of cultured cells by means of the patch-clamp technique, whole cell patch clamp recordings of a cortical neuron: (a) current clamp mode (CC), voltage responses to a current pulse of $+50 \text{ pA}$, $E_m = -47 \text{ mV}$, $I_{\text{hold}} = -30 \text{ pA}$, $V_{\text{hold}} \sim -70 \text{ mV}$ and (b) voltage clamp mode (VC), current responses of the same cell induced by stepwise application of 10 mV voltage stimuli (-100 – 100 mV), $V_{\text{hold}} = -60 \text{ mV}$. Cell growth was guided by means of $\text{A}\mu\text{CP}$ with PL/ECM, DIV 10.

probability of the channel opening after binding a neurotransmitter molecule (Johnston & Miao-Sun 1995). An additional fact, which adds to the complexity of this relatively 'simple' model system, is that the neuronal cells were connected in networks and activity of the neighbouring cells could contribute to the response of the recorded cell. Thus, the experiments show geometrically defined reconstruction of neuronal networks on silicon chips in alignment with the microstructured features on the chip surface and their interface to microfluidics. The extracellular environment of recorded neuronal cells in networks was manipulated by spatially resolved, non-invasive neurotransmitter application, while physiological

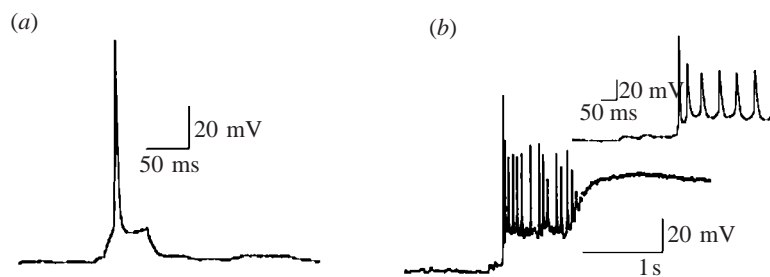


Figure 9. Whole cell patch clamp recordings of a cortical neuron, DIV 14: (a) CC, voltage response to a current pulse of 100 pA, $E_m = -60$ mV, $I_{hold} = -18$ pA, $V_{hold} \sim -70$ mV and (b) chemical (non-invasive) stimulation of the same cell with neurotransmitter glutamate delivered via the microfluidic system, $I_{hold} = -14$ pA, $V_{hold} = -68$ mV; flow rate 0.3 ml min^{-1} , 10 mM glutamate and 5 μM glycine in the stimulation solution ES2. The insert shows a part of the recording corresponding to the interval 7.9–8.5 s.

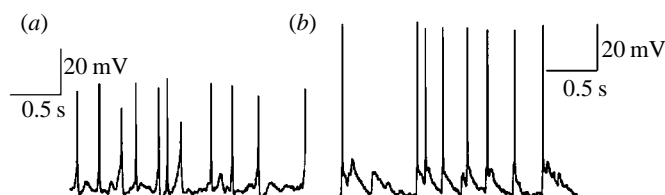


Figure 10. Whole cell patch clamp recordings of a cortical neuron, DIV 13: (a) $E_m = -44$ mV, $I_{hold} = -14$ pA and (b) chemical stimulation of the same cell with glutamate via the microfluidic system, flow rate 0.3 ml min^{-1} , 10 mM glutamate and 5 μM glycine in the stimulation solution ES2. Changes in the kinetics of the recordings are probably due to the activation of glutamate receptor ion channels.

functionality of the neurons in the on-chip reconstructed neural network was preserved. Such a system will be further employed for the investigation of the influence of localized chemical gradients on network formation and long-term modulation. For further studies, advanced methodologies based on electrokinetic effects in microfluidic systems would be advantageous to control the delivery of solutions.

5. CONCLUSIONS

We developed a biohybrid system, in which neuronal networks were reconstructed on microstructured silicon chips and interfaced to microfluidics. A high degree of geometrical control over the network architecture and alignment of the network with the substrate features was achieved by means of $\text{A}\mu\text{CP}$. The extracellular environment of recorded neuronal cells in networks was manipulated by spatially resolved, non-invasive neurotransmitter application, while physiological functionality of the neurons in the on-chip reconstructed neural network was preserved. A modular design of the device allows for culturing neuronal cells on-chips under standard cell culture conditions. Such a system will be useful for the investigation of the influence of localized chemical gradients on network formation and long-term modulation. This approach is promising for the integration with on-chip cell culture systems and microelectrode arrays for physiological and pharmacological assays, as well as for cell differentiation studies.

The authors thank R. Helpenstein for the help with neuronal cell culture.

REFERENCES

- Aebersold, R. & Mann, M. 2003 Mass spectrometry-based proteomics. *Nature* **422**, 198–207. ([doi:10.1038/nature01511](https://doi.org/10.1038/nature01511))
- Berdondini et al. In press. *Sens. Actuators B*, available online 28 June 2005.
- Bliss, T. V. P. & Collingridge, G. L. 1993 A synaptic model of memory: long-term potentiation in the hippocampus. *Nature* **361**, 31–39. ([doi:10.1038/361031a0](https://doi.org/10.1038/361031a0))
- Bliss, T. V. & Gardner-Medwin, A. R. 1973 Long-lasting potentiation of synaptic transmission in the dentate area of the unanaesthetized rabbit following stimulation of the perforant path. *J. Physiol.* **232**, 357–374.
- Bortolotto, Z. A., Bashir, Z. I., Davies, C. H. & Collingridge, G. L. 1994 A molecular switch activated by metabotropic glutamate receptors regulates induction of long-term potentiation. *Nature* **368**, 740–743. ([doi:10.1038/368740a0](https://doi.org/10.1038/368740a0))
- Brewer, G. J., Torrichelli, J. R., Evege, E. K. & Price, P. J. 1993 Optimized survival of hippocampal neurons in B27 supplemented Neurobasal, a new serum-free medium combination. *J. Neurosci. Res.* **35**, 567–576. ([doi:10.1002/jnr.490350513](https://doi.org/10.1002/jnr.490350513))
- Brüggemann, A., George, M., Klau, M., Beckler, M., Steindl, J. & Fertig, N. 2003 High quality ion channel analysis on a chip with the NPC technology. *Assay Drug Dev Technol.* **1**, 665–673. ([doi:10.1089/154065803770381020](https://doi.org/10.1089/154065803770381020))
- Chang, C. J., Brewer, G. J. & Wheeler, B. C. 2001 Modulation of neural network activity by patterning. *Biosens. Bioelectron.* **16**, 527–533. ([doi:10.1016/S0956-5663\(01\)00166-X](https://doi.org/10.1016/S0956-5663(01)00166-X))
- Claverol-Tinture, E. & Pine, J. 2002 Extracellular potentials in low-density dissociated neuronal cultures. *J. Neurosci.* **117**, 13–21.

Cull-Candy, S., Brickley, S. & Farrant, M. 2001 NMDA receptor subunits: diversity, development and disease. *Curr. Opin. Neurobiol.* **11**, 327–335. (doi:10.1016/S0959-4388(00)00215-4)

Egert, U., Schlosshauer, B., Fennrich, S., Nisch, W., Fejt, M., Knott, T. & Hämerle, H. 1998 A novel organotypic long-term culture of the rat hippocampus on substrate-integrated multielectrode arrays. *Brain Res. Protocols* **2**, 229–242. (doi:10.1016/S1385-299X(98)00013-0)

Eguchi, Y., Ogiue-Ikeda, M. & Ueno, Sh. 2003 Control of orientation of rat Schwann cells using an 8-T static magnetic field. *Neurosci. Lett.* **351**, 130–132. (doi:10.1016/S0304-3940(03)00719-5)

Eversmann, B. *et al.* 2003 A 128×128 CMOS biosensor array for extracellular recording of neural activity. *IEEE J. Solid State Circuits* **38**, 2306–2317. (doi:10.1109/JSSC.2003.819174)

Folch, A. & Toner, M. 2000 Microengineering of cellular interactions. *Annu. Rev. Biomed. Eng.* **02**, 227–256. (doi:10.1146/annurev.bioeng.2.1.227)

Fox, K., Henley, J. & Isaac, J. 1999 Experience-dependent development of NMDA receptor transmission. *Nature Neurosci.* **2**, 297–299. (doi:10.1038/7203)

Fromherz, P. 2003 Nanoelectronic interfacing: semiconductor chips with ion channels, nerve cells, and brain. In *Nanoelectronics and information technology* (ed. R. Waser), pp. 781–810. Berlin: Wiley–VCH.

Gross, G. W., Harsch, A., Rhoades, B. K. & Göpel, W. 1997 Odor, drug and toxin analysis with neuronal networks *in vitro*: extracellular array recording of network responses. *Biosens. Bioelectronics* **12**, 373–393. (doi:10.1016/S0956-5663(97)00012-2)

Hebb, D. O. 1949 *The organization of behavior: a neuropsychological theory*. New York: Wiley.

Issaq, H. J., Chan, K. C., Janini, G. M., Conrads, T. P. & Veenstra, T. D. 2005 Multidimensional separation of peptides for effective proteomic analysis. *J. Chromatogr. B* **817**, 35–47. (doi:10.1016/j.jchromb.2004.07.042)

Johnston, D. & Miao-Sun, W. D. 1995 *Foundations of cellular neurophysiology*, p. 676. Boston, MA: Massachusetts Institute of Technology.

Kandel, E. R., Schwartz, J. H. & Jessel, T. M. (eds) 2000 *Principles of neural science*, p. 1414, 4th edn. New York: McGraw Hill.

Kaul, R. A., Syed, N. J. & Fromherz, P. 2004 Neuron-semiconductor chip with chemical synapses between identified neurons. *Phys. Rev. Lett.* **92**, 038 102–1–038 102-4. (doi:10.1103/PhysRevLett.92.038102)

Li, J., Tremblay, T. L., Harrison, D. J. & Thibault, P. 2002 Application of microfluidic devices to proteomics research: identification of trace-level protein digests and affinity capture of target peptides. *Mol. Cell. Proteomics* **1**, 157–168. (doi:10.1074/mcp.M100022-MCP200)

Lion, N. *et al.* 2003 Microfluidic systems in proteomics. *Electrophoresis* **24**, 3533–3562. (doi:10.1002/elps.200305629)

Lu, X., Huang, W. H., Wang, Z. L. & Cheng, J. K. 2004 Recent developments in single-cell analysis. *Anal. Chim. Acta* **510**, 127–138. (doi:10.1016/j.aca.2004.01.014)

Ludvig, N., Potter, P. E. & Fox, S. E. 1994 Simultaneous single-cell recording and microdialysis within the same brain site in freely behaving rats: a novel neurobiological method. *J. Neurosci. Meth.* **55**, 31–40. (doi:10.1016/0165-0270(94)90037-X)

Maher, M. P., Pine, J., Wright, J. & Tai, Yu-Ch. 1999 The neurochip: a new multielectrode device for stimulating and recording from cultured neurons. *J. Neurosci. Meth.* **87**, 45–56. (doi:10.1016/S0165-0270(98)00156-3)

Matsue, T. 2005 On-chip gene engineering based on electrochemical detection. In *Joint Meeting Bioelectrochemistry*, Coimbra, Portugal 19–24 June, 2005.

Merz, M. & Fromherz, P. 2005 Silicon chip interfaced with a geometrically defined net of snail neurons. *Adv. Funct. Mater.* **15**, 739–744.

Mohanty, S. K., Sharma, M., Panicker, M. M. & Gupta, P. K. 2005 Controlled induction, enhancement, and guidance of neuronal growth cones by use of line optical tweezers. *Opt. Lett.* **30**, 2596–2598.

Morin, F., Nishimura, N., Griscom, L., LePoufle, B., Fujita, H., Takamura, Y., & Tamiya, E. In press Constraining the connectivity of neuronal networks cultured on microelectrode arrays with microfluidic techniques: a step towards neuron-based functional chips. *Biosens. Bioelectronics*, available online 14 June 2005.

Mourzina, Y., Mai, T., Poghossian, A., Ermolenko, Yu., Yoshinobu, T., Vlasov, Y., Iwasaki, H. & Schöning, M. J. 2003 K-selective field-effect sensors as transducers for bioelectronic applications. *Electrochimica Acta* **48**, 3333–3339. (doi:10.1016/S0013-4686(03)00402-X)

Mourzina, Iou, Steffen, A., Kalyaguine, D., Carius, R. & Offenhäusser, A. 2005 Capillary zone electrophoresis of amino acids on a hybrid poly(dimethylsiloxane)-glass chip. *Electrophoresis* **26**, 1849–1860. (doi:10.1002/elps.200410295)

Nagamine, K., Onodera, Sh., Torisawa, Y., Yasukawa, T., Shiku, H. & Matsue, T. 2005 On-Chip transformation of Bacteria. *Anal. Chem.* **77**, 4278–4281. (doi:10.1021/ac048278n)

Neher, E. 2001 Molecular biology meets electronics. *Nat. Biotechnol.* **19**, 114. (doi:10.1038/84359)

O'Connor, J. J., Rowan, M. J. & Anwyl, R. 1994 Long-lasting enhancement of NMDA receptor-mediated synaptic transmission by metabotropic glutamate receptor activation. *Nature* **367**, 557–559. (doi:10.1038/367557a0)

Oliva, A. A., James, C. D., Kingman, C. E., Craighead, H. G. & Bunker, G. A. 2003 Patterning axonal guidance molecules using a novel strategy for microcontact printing. *Neurochem. Res.* **28**, 1639–1648. (doi:10.1023/A:1026052820129)

Otto, F., Götz, Ph., Fleischer, W. & Siebler, M. 2003 Cryopreserved rat cortical cells develop functional neuronal networks on microelectrode arrays. *J. Neurosci. Meth.* **128**, 173–181. (doi:10.1016/S0165-0270(03)00186-9)

Offenhäusser, A. & Knoll, W. 2001 Cell–transistor hybrid systems and their potential applications. *TRENDS Biotechnol.* **19**, 62–66. (doi:10.1016/S0167-7799(00)01544-4)

Peng, J., Kim, M. J., Cheng, D., Duong, D. M., Gygi, S. P. & Sheng, M. 2004 Semiquantitative proteomic analysis of rat forebrain postsynaptic density fractions by mass spectrometry. *J. Biol. Chem.* **279**, 21 003–21 011. (doi:10.1074/jbc.M400103200)

Peterman, M. C., Noolandi, J., Blumenkranz, M. & Fishman, H. A. 2004 Localized chemical release from an artificial synapse chip. *PNAS* **101**, 9951–9954. (doi:10.1073/pnas.0402089101)

Pihl, J., Sinclair, J., Sahlin, E., Karlsson, M., Petterson, F., Olofsson, J. & Orwar, O. 2005 Microfluidic gradient-generating device for pharmacological profiling. *Anal. Chem.* **77**, 3897–3903. (doi:10.1021/ac050218+)

Pine, J. 1980 Recording action-potentials from cultured neurons with extracellular microcircuit electrodes. *J. Neurosci. Meth.* **2**, 19–31. (doi:10.1016/0165-0270(80)90042-4)

Popescu, G. & Auerbach, A. 2004 The NMDA receptor gating machine: lessons from single channels. *Neuroscience* **10**, 192–198. (doi:10.1177/1073858404263483)

Rhee, S. W., Taylor, A. M., Tu, C. H., Cribbs, D. H., Cotman, C. W. & Jeon, N. L. 2005 Patterned cell culture inside microfluidic devices. *Lab Chip* **5**, 102–107. (doi:10.1039/b403091e)

Santini, J. T., Cima, M. J. & Langer, R. 1999 A controlled-release microchip. *Nature* **397**, 335–338. (doi:10.1038/16898)

Stetts, A., Bucher, V., Burkhardt, C., Weber, U. & Nisch, W. 2003 Patch-clamping of primary cardiac cells with micro-openings in polyimide films. *Med. Biol. Eng. Comput.* **41**, 223–240.

Sugio, Y., Kojima, K., Moriguchi, H., Takahashi, K., Kaneko, T. & Yasuda, K. 2004 An agar-based on-chip neural-cell-cultivation system for stepwise control of network pattern generation during cultivation. *Sens. Actuators B* **99**, 156–162. (doi:10.1016/S0925-4005(03)00550-1)

Szili, E., Thissen, H., Hayes, J. P. & Voelker, N. 2004 A biochip platform for cell transfection assays. *Biosens. Bioelectron.* **19**, 1395–1400. (doi:10.1016/j.bios.2003.12.019)

Takoh, K., Ishibashi, T., Matsue, T. & Nishizawa, M. 2005 Localized chemical stimulation of cellular micropatterns using a porous membrane-based culture substrate. *Sens. Actuators B* **108**, 683–687. (doi:10.1016/j.snb.2004.12.090)

Vogt, A. K., F, D., Stefani, A., Best, G., Nelles, A., Yasuda, W., Knoll, W. & Offenhäusser, A. 2004 Impact of micropatterned surfaces on neuronal polarity. *J. Neurosci. Meth.* **134**, 191–198. (doi:10.1016/j.jneumeth.2003.11.004)

Vogt, A. K., Wrobel, G., Meyer, W., Knoll, W. & Offenhäusser, A. 2005 Synaptic plasticity in micropatterned neuronal networks. *Biomaterials* **26**, 2549–2557. (doi:10.1016/j.biomaterials.2004.07.031)